

## Interplay between jamming and percolation upon random sequential adsorption of competing dimers and monomers

Federica Rampf\* and Ezequiel V. Albano

*Instituto de Investigaciones Físicoquímicas Teóricas y Aplicadas (INIFTA), CONICET, UNLP, Sucursal 4, Casilla de Correo 16, (1900) La Plata, Argentina*

(Received 22 August 2002; published 30 December 2002)

The competitive random coadsorption of dimers and monomers, with probabilities  $P_D$  and  $P_M$ , such as  $P_D + P_M = 1$ , respectively, is studied numerically by means of Monte Carlo simulations. Excluded volume and nearest-neighbor infinite repulsion between unlike species is considered. The subtle interplay between competitive coadsorption, jamming behavior and the emergency of percolation clusters is analyzed in detail. Taking  $P_M$  as the single parameter of the model, five characteristic regions where the system exhibit different physical behavior can be identified: I) For  $P_M \leq P_{M1} \approx 0.4025(25)$  the standard percolation of dimers is observed; II) Within the interval  $P_{M1} < P_M < P_{M1}^* \approx 0.4375(25)$  clusters of all species (monomers, dimers, and empty sites) are finite (nonpercolating); III) For  $P_{M1}^* \leq P_M \leq P_{M2}^* \approx 0.5425(25)$  the percolation of homogeneous clusters of empty sites is observed; IV) Within the interval  $P_{M2}^* < P_M < P_{M2} \approx 0.5575(25)$ , the system behaves as in Region II; and finally, V) For  $P_{M2} \leq P_M$ , one has the standard percolation of monomers.

DOI: 10.1103/PhysRevE.66.061106

PACS number(s): 02.50.Ey, 64.60.Ak, 05.40.-a

### I. INTRODUCTION

The study of the physical and chemical properties of adsorbed monolayers is a topic that has been attracting considerable attention for many years [1–6]. The equilibrium state of such overlayers can be described by a Gibbs measure parametrized by the coverage  $\theta$  and the temperature  $T$ . In particular the critical behavior of adsorbed films has extensively studied, see, e.g., Refs. [6–8]. Another quite interesting scenario is the irreversible adsorption of atoms and molecules on solid surfaces. Here, the term irreversible actually means that the relaxation time scale of the deposition process is much longer than the time required to form the whole deposit. Under these conditions the system evolves rapidly toward far-from equilibrium conditions and the dynamics becomes essentially dominated by geometrical exclusion effects between particles. This kind of effects has been observed in numerous experiments, for a review, e.g., Ref. [9].

From the theoretical point of view, irreversible adsorption has successfully been studied assuming the sequential adsorption of particles within a lattice gas framework, so that the state of the sites on the lattice is assumed to change irreversibly from empty to occupied states [10–13]. In the simplest approach adsorption sites are chosen at random leading to the process known as random sequential adsorption (RSA). In a more general approach the adsorption rates depend on the environment of the adsorption site leading to the so called cooperative sequential adsorption (CSA), for an excellent review on these topics see, e.g., Ref. [13]. If either RSA or CSA involve adsorption on single sites, the case is termed “monomer filling.” Also, processes involving adjacent pairs of sites are referred as “dimer filling,” while adsorption on larger ensembles of sites corresponds to “animal filling” [13]. RSA and CSA are appropriated approaches for modeling many physical, chemical, and biological processes

where the microscopic steps are irreversible and equilibration is not possible during the time scale of the experiment, for various examples see, e.g., Refs. [9–22].

The aim of this manuscript is to study, by means of numerical Monte Carlo simulations, the CSA of monomers and dimers. In the case treated here, the local environment of each site is modified by the operation of short range (infinite) repulsion between unlike species. Our study is motivated by the cooperative adsorption of CO and O<sub>2</sub> molecules on single crystal surfaces. Here, CO is assumed to be the monomer since it bounds to the metal surface through the carbon atom occupying a single site on the surface. In contrast, O<sub>2</sub> is the dimer because upon adsorption it dissociates into two atoms blocking two sites of the surface [23,24]. The CSA of CO and O<sub>2</sub> is the first step of the catalytic oxidation of CO that leads desorbed CO<sub>2</sub>. It should be mentioned that such a reaction has been modeled by means of a dimer-monomer lattice gas reaction model [25].

In addition to the interest of monomer-dimer systems for the understanding of the early stages of simple catalytic reactions, the interplay between RSA and percolation is relevant for the description of the many physical, chemical, and even biological systems. For reviews on the theory and application of percolation see, e.g., Refs. [26–28]. Within this context, the study of the percolation properties of both dimers and monomers is another goal of the present work. It is shown that the constraint of CRA causes the occurrence of percolation windows that are characterized in detail.

It should be mentioned that the understanding of the interplay between RSA and percolation is also a topic of great interest that has been addressed by various authors, see, e.g., Refs. [29–32] (for a review see, also, Ref. [13]). However, within our best knowledge such interplay has not been studied yet for the case of the competitive coadsorption of dimers and monomers, as proposed in the present paper.

The manuscript is organized as follows: in Sec. II the model for RSA of dimers and monomers is defined and the simulation method is described. Results are presented and

\*Present address: Institut für Physik, Johannes Gutenberg Universität Mainz, Staudinger Weg 7, 55099 Mainz, Germany

discussed in Sec. III, while our conclusions are stated in Sec. IV.

## II. THE MODEL AND THE SIMULATION METHOD

The RSA of two competitive species, namely dimers and monomers, is simulated on the square lattice assuming periodic boundary conditions and using samples of side  $L$  ( $32 \leq L \leq 1024$ ), where distances are measured in lattice units (LU). Apart from the excluded volume interaction, infinite repulsion between unlike species adsorbed on nearest-neighbor (NN) sites is also considered. In other words, adsorption of dimers and monomers on adjacent sites is forbidden.

To implement the competitive RSA, monomers are selected at random with probability  $P_M$ , while dimers are chosen with probability  $P_D$ . Setting  $P_M + P_D = 1$ , the model has a single parameter, namely,  $P_M$ . Furthermore, adsorption sites are also selected at random. Monomers are always adsorbed on empty sites provided the absence of dimers already adsorbed around the four NN sites. The latter requirement accounts for the infinite repulsion. After selection of a dimer and an empty site, one has also to select at random an NN site of the previously selected one. If this additional site is empty the dimer is adsorber provided the absence of monomers already adsorbed on any of the six NN sites of the selected ones.

In order to study the jamming behavior of the system each run is finished when further adsorption is no longer possible, i.e., when the jamming coverage is reached. (Notice that the coverage is measured in units of particles per unit area.) In these cases one typically has the lattice covered by a certain density of monomers ( $\theta_M^J$ ) and dimers ( $\theta_D^J$ ), while due to the infinite repulsion and the geometrical constrain between dimers one may also have a certain density of empty sites ( $\theta_E^J$ ).

On the other hand, in order to study the percolative behavior of the adsorbed species, the standard HK algorithm is used [33]. Starting from an empty lattice the onset of a percolation cluster is detected upon both, monomer and dimer adsorption. For this kind of study, each run ends when the first percolation cluster is identified. Subsequently, the coverage of the percolating species is evaluated. Let  $\theta_i^{PX}$  ( $X = M, D, E$ , for monomer, dimer, and empty sites, respectively) be, such a coverage measured for the  $i$ th run. Then, the average value is given by

$$\theta^{PX} = \frac{1}{N_R} \sum \theta_i^{PX} \quad (1)$$

and the corresponding fluctuations are given by

$$\sigma \theta^{PX} = \sqrt{\frac{1}{N_R} \sum (\theta^{PX} - \theta_i^{PX})^2}, \quad (2)$$

where  $N_R$  is the number of runs. Typically averages are taken over  $10^2 \leq N_R \leq 10^3$ , depending on the lattice size.

According to the standard finite-size scaling theory of percolation, it is expected that [26]

$$\theta^{PX}(L) = \theta^{PX}(\infty) + AL^{-1/\nu_X}, \quad (3)$$

where  $\theta^{PX}(L)$  is the  $L$ -dependent percolation threshold,  $\theta^{PX}(\infty)$  is the  $L = \infty$  percolation threshold and  $\nu_X$  is the correlation length exponent. Furthermore, it is known that the fluctuations scale as [26]

$$\sigma \theta^{PX} \sim L^{-1/\nu_X}. \quad (4)$$

So, determining  $\nu_X$  with the aid of Eq. (4) it is also possible to evaluate the percolation threshold in the thermodynamic limit using Eq. (3).

Furthermore, the probability of a particle to belong to the incipient percolating cluster  $P_\infty^X(L)$ , behaves as [26]

$$P_\infty^X(L) = L^{-\beta/\nu}, \quad (5)$$

where  $\beta$  is the order parameter critical exponent.

It should be noticed that the universality class of random percolation in  $d=2$  dimensions is very well identified and the critical exponents are known exactly, namely,  $\nu=4/3$  and  $\beta=5/36$  [26]. Therefore, based on the well established concept of universality that applies to second-order phase transitions, it is expected that both percolation of monomers and dimers, at the percolation threshold, would belong to the universality class of random percolation. Of course, the repulsive interaction between dimers and monomers that is explicitly considered in the present paper would influence the local structure of the clusters. However, such an interaction is of short range and consequently the typical length of the interaction range becomes negligible as compared to the (diverging) correlation length at criticality. In this way, local details due to the interaction are washed out and the universality class of random percolation will prevail. However, as anticipated in the preceding sections, the interplay between jamming and percolation leads to the occurrence of nonpercolating phases. Therefore, it is still interesting to evaluate the critical exponents for percolation just at the limit between phases, in order to check if the properties of the universality class of random percolation prevails over the constraint imposed by the jamming process.

## III. RESULTS AND DISCUSSION

The time evolution of  $\theta^X$  ( $X = M, D$ , and  $E$ ) has been followed for a large number of values of the parameter  $P_M$  and for long enough time. In all cases the systems reach a jamming coverage where further adsorption is no longer possible. In this manuscript we will focus our attention to the dependence of the jamming coverage on  $P_M$ .

Figure 1 shows plots of  $\theta_M^J$ ,  $\theta_D^J$ , and  $\theta_E^J$  vs  $P_M$ . For  $P_M = 0$  the well known jamming coverage of isolated dimers is recovered, namely,  $\theta_{ID}^J \cong 0.906$ . Subsequently,  $\theta_D^J$  decreases monotonically when increasing  $P_M$ , while  $\theta_M^J$  follows the opposite trend. Of course,  $\theta_M^J = 1$  is obtained for  $P_M = 1$ . It is also observed that  $\theta_M^J = \theta_D^J$  close to  $P_M \cong 0.493$ . Also, just for this value of the parameter,  $\theta_E^J$  reaches a maximum.

According to Fig. 1, it may be expected that for smaller

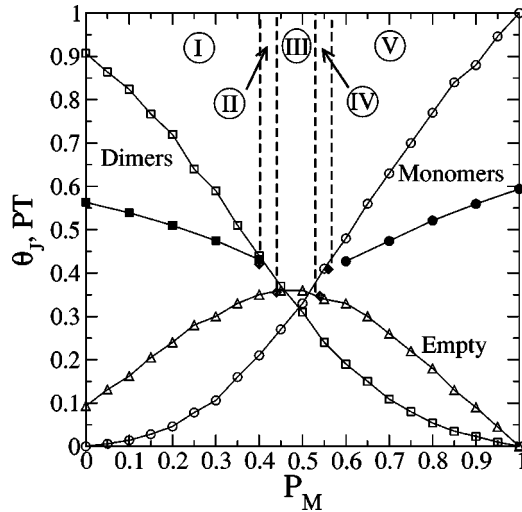


FIG. 1. Plots of the jamming coverages for monomers, dimers, and empty sites  $\theta_M^j$ ,  $\theta_D^j$ , and  $\theta_E^j$ , respectively, vs  $P_M$ , as obtained using lattices of side  $L=512$  LU. Notice that coverages are measured in units of particles per unit area. Results are averaged over  $10^2$  different samples. Full squares at the left hand side (circles at the right hand side) show the percolation thresholds for dimers (monomers) as obtained extrapolating finite size results to the thermodynamic limit. Five regions (I–V) where the system exhibits different percolation properties are shown in the figure and discussed in the text.

(larger) values of  $P_M$  one would observe percolation clusters of dimers (monomers), while for  $P_M \approx 0.5$  the high density of empty sites may eventually prevent percolation of these species. In fact, Fig. 2 shows typical snapshot configurations obtained for three different values of  $P_M$ . For  $P_M=0.20$ , the percolation of dimers, which is the majority species, can clearly observed [Fig. 2(a)]. Also, for  $P_M=0.80$ , the percolation of monomers is observed [Fig. 2(b)]. Finally, for  $P_M=0.50$  neither monomers nor dimers can percolate, but the percolation of empty sites is verified [Fig. 2(c)].

Consequently, using Eqs. (3) and (4),  $\theta_M^p(L)$  and  $\sigma\theta_M^p(L)$ , as well as  $\theta_D^p(L)$  and  $\sigma\theta_D^p(L)$ , have been evaluated for  $P_M < 0.5$  and  $P_M > 0.5$ , respectively. Also,  $\theta_E^p(L)$  and  $\sigma\theta_E^p(L)$  have been evaluated close to  $P_M \approx 0.5$ . Figure 3 shows log-log plots of  $\sigma\theta^{pX}$  ( $X=M, D, E$ ) vs  $L$ . The best fits of the data give:  $1/\nu_M \approx 0.754$ , i.e.,  $\nu_M = 1.33$  for monomers and  $1/\nu_D \approx 0.722$ , i.e.,  $\nu_D = 1.38$  for dimers, respectively. On the other hand, for  $P_M \approx 0.5$  the percolation of empty sites with  $1/\nu_E \approx 1.03 \pm 0.03$ , i.e.,  $\nu_E \approx 0.975$  is observed. Similar plots performed for different values of  $P_M$  lead us to estimate that the correlation length exponents for percolation of both dimers and of monomers are close to  $\nu_D \approx \nu_M \approx 4/3$ , as expected for random percolation. Furthermore, for the percolation of empty sites one has  $\nu_E \approx 1.0$ .

Using these values of the correlation length exponents and with the aid of Eq. (3) the critical thresholds for the percolation of monomers and dimers in the thermodynamic limit ( $L \rightarrow \infty$ ) have been evaluated. The obtained results are shown in Fig. 1. At the right hand side of Fig. 1, where monomers is the majority species, one observes that the threshold for  $P_M = 1$  is close to  $\theta_M^p(P_M=1) \approx 0.593$  in agreement with the

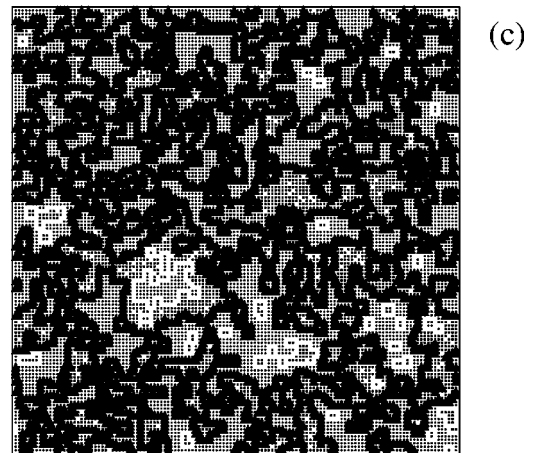
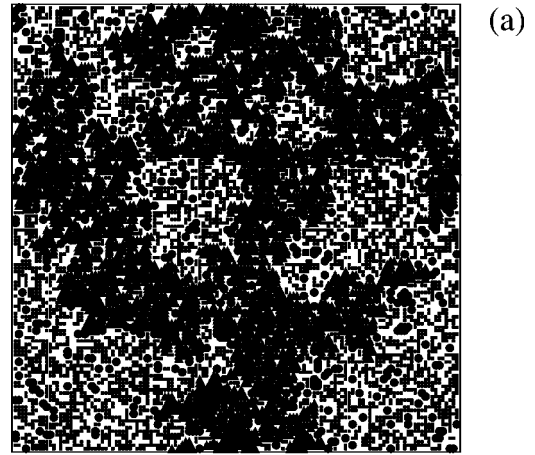


FIG. 2. Typical snapshot configurations of jammed samples as obtained using lattices of side  $L=128$ . (a)  $P_M=0.20$ . Full circles, squares, and triangles correspond to monomers, dimers, and the percolating cluster of dimers, respectively. (b)  $P_M=0.80$ . Full circles, squares, and triangles correspond to monomers, dimers, and the percolating cluster of monomers, respectively. (c)  $P_M=0.50$ . Full circles, squares, and triangles correspond to monomers, dimers, and the percolating cluster of empty sites, respectively.

already known percolation threshold of classic percolation given by  $P_C=0.5927460(5)$  [34]. However, when the coadsorption with dimers is considered, the critical threshold monotonically decreases and close to  $P_{M2} \approx 0.56$  one has the

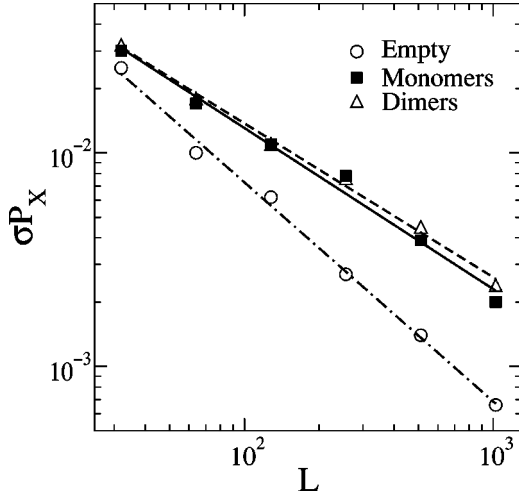


FIG. 3. Log-log plots of  $\sigma\theta_X^P(L)$  (with  $X=M, D$ , and  $E$ ) vs  $L$ , measured in LU. The lines show the best fits of the data. Results are averaged over  $10^2$  different samples.

intersection with the jamming curve, namely,  $\theta_M^J = \theta_M^P$ . Notice that for  $P_M < P_{M2}$  monomers do not percolate anymore.

Considering percolation of dimers, left hand side of Fig. 1, one observes a qualitatively similar behavior. In fact, for  $P_M = 0$  the value  $\theta_D^P(P_M = 0) \cong 0.562$ , corresponding to the percolation threshold for adsorption of isolated dimers is recovered [13]. Also,  $\theta_D^P$  decreases monotonically when  $P_M$  is increased up to the intersection with the jamming curve that occurs close to  $P_{M1} \cong 0.40$ , such as for  $P_M > P_{M1}$  the percolation of dimers is no longer observed.

The observation of a window along the  $P_M$  axis such as for  $P_{M1} \leq P_M \leq P_{M2}$  neither monomers nor dimers can percolate, is physically plausible in light of the results shown in Fig. 1. In fact, above  $P_{M1}$  the percolation of dimers would require a dimer density higher than that allowed by the dynamic competition with monomers and consequently percolation is no longer possible. A similar argument can be drawn close to  $P_{M2}$  for monomer's percolation. The occurrence of a nonpercolation window for dimers and monomers nicely emerges due to the interplay between dynamically competitive coadsorption of different species and the coverage constraints imposed by the percolation process.

In order to locate more accurately the window, the percolation probabilities (PP), of both dimers and monomers, have been recorded for different values of  $P_M$  and the lattice size. As shown in Fig. 4, for the case of monomers one has that  $PP^M$  increases (decreases) for  $P_M > 0.560$  ( $P_M < 0.555$ ) an observation that lead us to estimate  $P_{M2} = 0.5575 \pm 0.0025$ . Similarly, for the case of dimers (not shown here for the sake of space) it is found that  $PP^D$  tends to decrease (increase) for  $P_M < 0.405$  ( $P_M > 0.400$ ) as  $L \rightarrow \infty$ . So, our estimation of the lower limit of the window is  $P_{M1} = 0.4025 \pm 0.0025$ .

The probability of a particle to belong to the incipient percolating cluster of the same species  $P_\infty^X(L)$  ( $X=D, M, E$ ), has also been evaluated and analyzed. Figure 5 shows log-log plots of  $P_\infty(L)$  vs  $L$ . From the slopes of these plots, as well as a set of similar ones not shown here for the sake of space, the following values are obtained:

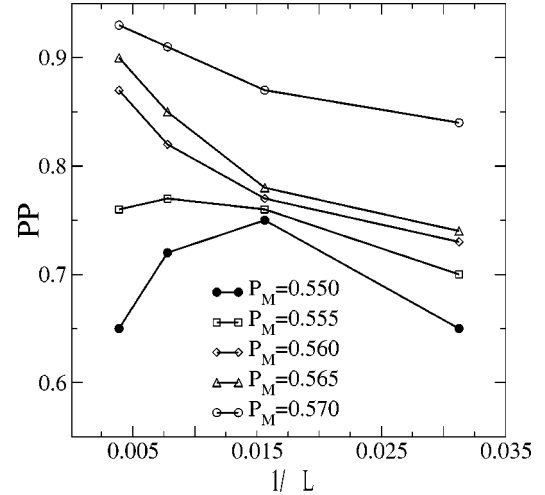


FIG. 4. Plots of the percolation probability (PP) of monomers vs  $1/L$ , measured in  $\text{LU}^{-1}$  obtained for different values of  $P_M$  as indicated in the figures. The lines are drawn to guide the eyes.

$$\beta_M / \nu_M \cong 0.132 \pm 0.020, \quad \beta_D / \nu_D \cong 0.136 \pm 0.020. \quad (6)$$

Our findings for both, dimers and monomers, are consistent with the value  $\beta/\nu = 5/48 \cong 0.104$ , corresponding to the universality class of standard percolation [26]. So, based on the evaluation of the exponents  $\nu$  and  $\beta/\nu$  it is concluded that clusters of both, dimers and monomers, even at the limit of the percolation window given by  $P_{M1}$  and  $P_{M2}$ , respectively, belong to the universality class of standard percolation.

The analysis of the behavior of the empty sites within the window allow us to detect their percolation close to  $P_M = 0.5$  [see, e.g., Fig. 2(c)]. The evaluation of the exponents using the plots  $\sigma\theta_E^P$  and  $P_\infty^E$  vs  $L$ , as shown in Figs. 3 and 5, respectively, gives

$$1/\nu_E = 1.026 \pm 0.030, \quad \beta_E / \nu_E = 0.007 \pm 0.010. \quad (7)$$

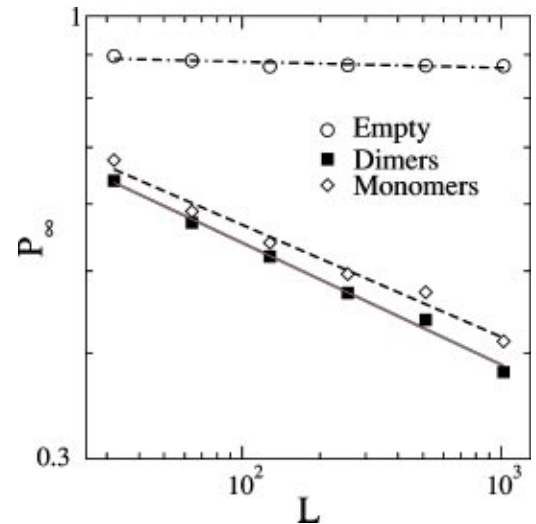


FIG. 5. Log-log plots of  $P_\infty(L)$  vs  $L$ , measured in LU. The lines show the best fits of the data corresponding to empty sites, dimers, and monomers as indicated in the figure.

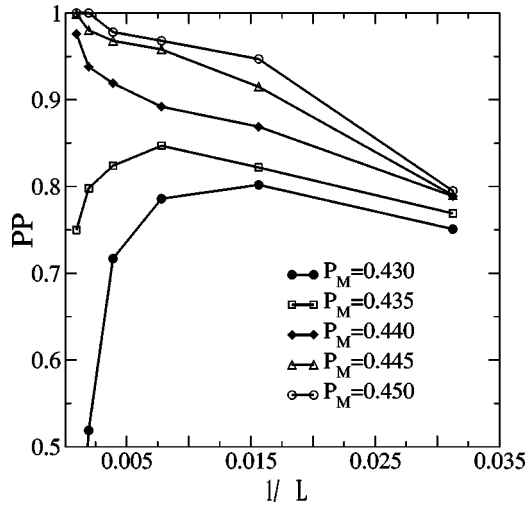


FIG. 6. Plots of the percolation probability (PP) vs  $1/L$ , measured in  $\text{LU}^{-1}$ , obtained for different values of  $P_M$  as indicated in the figures. The lines are drawn to guide the eyes and the data were obtained close to  $P_{M1}^*$ .

These exponents are consistent with the formation of homogeneous clusters of fractal dimension  $D_F = d - \beta/\nu = d = 2$ . So, percolation clusters of empty sites are compact objects in agreement with the fact that such clusters are measured above the percolation threshold. On the other hand, clusters of both dimers and monomers, at the percolation threshold, are fractal self-similar objects of dimension  $D_F = d - \beta/\nu \cong 1.89$ .

Performing an even deeper analysis of behavior of empty sites within the window  $P_{M1} < P_M < P_{M2}$ , it is found that empty sites percolate close to the center of the window while approaching the limits of the window only finite (nonpercolating) clusters of all species (dimers, monomers, and empty sites) are found. So, it is concluded that there are two additional critical points ( $P_{M1}^*$  and  $P_{M2}^*$ , respectively) such as  $P_{M1} < P_{M1}^* < P_{M2}^* < P_{M2}$ . Therefore, five different Regions, each of them exhibiting a characteristic percolative behavior, can clearly be identified as follows (see Fig. 1):

*Region I.* For  $P_M < P_{M1}$  one observes standard percolation of dimers.

*Region II.* Within the interval  $P_{M1} < P_M < P_{M1}^*$  clusters of all species (monomers, dimers, and empty sites) are finite (nonpercolating).

*Region III.* For  $P_{M1}^* < P_M < P_{M2}^*$  the percolation of homogeneous clusters of empty sites is observed.

*Region IV.* Within the interval  $P_{M2}^* < P_M < P_{M2}$ , the system behaves as in Region II.

*Region V.* For  $P_{M2} < P_M$ , one has the standard percolation of monomers.

In order to locate more accurately both  $P_{M1}^*$  and  $P_{M2}^*$  the percolation probability of empty sites has been evaluated for different values of  $P_M$  and using lattices of various sizes. As shown in Fig. 6, the lower threshold for percolation of empty sites is estimated to be  $P_{M1}^* = 0.4375 \pm 0.0025$ . Also, the upper threshold can be evaluated drawing a similar figure (not shown here for the sake of clarity) giving  $P_{M2}^* = 0.5425$

$\pm 0.0025$ . So, within the interval  $P_{M1}^* < P_M < P_{M2}^*$  (Region III), only homogeneous percolating clusters of empty sites are observed, such as  $D_F = d = 2$  and  $\nu_E = 1$ . In this Region one has that  $P_M \approx P_D \approx 0.5$ , so both species have almost the same probability of becoming selected during each adsorption trial. However, this window is not symmetric around  $P_M = 1/2$ , but instead one has  $|P_{M1}^* - 1/2| > P_{M2}^* - 1/2$ , reflecting the fact that monomers can be adsorbed straightforwardly on empty sites while dimers require two nearest-neighbor empty sites for adsorption. The competition between species with  $P_M \approx P_D$  and the operation of repulsion between unlike species favors the formation of islands of both dimers and monomers. These islands are surrounded by empty sites forming clusters such as one of them percolates. It is interesting to remark that percolation of empty sites is observed in spite of their low density ( $\theta_E \approx 0.43$  for  $P_M \cong 0.493$ , see Fig. 1) as compared to the percolation density for random percolation given by  $P_C = 0.5927460(5)$  [34]. Even for such a low density, the fact that  $D_F = 2$  points out that percolation clusters of empty sites are above the percolation threshold.

#### IV. CONCLUSIONS

Based on a numerical study of the competitive coadsorption of dimers and monomers on the square lattice it is concluded that the system exhibits a subtle interplay between jamming and percolation. For low values of  $P_M$  [i.e.,  $P_M < P_{M1} \approx 0.4025(25)$ ] only the percolation of dimers takes place. Incipient percolation clusters of dimers belongs to the universality class of standard percolation as follows from the evaluated critical exponents through a finite size scaling treatment of the numerical data. When  $P_M$  is increased up to  $P_{M1}^* \approx 0.4375(25)$  one observes finite (no-percolation clusters) of all species, including empty sites. This behavior is due to the constraint imposed by the competitive coadsorption on the density of dimers, that lies below the threshold necessary for the onset of percolation clusters. Subsequently, a window ( $P_{M1}^* < P_M < P_{M2}^* \approx 0.5425$ ) is identified, such as empty sites is the dominant species. Consequently, the percolation of homogeneous clusters of empty sites is observed. Due to a further increase of  $P_M$  until  $P_{M2} \approx 0.5575(25)$ , the competition between species does not allow the development of any percolation cluster. Finally, for  $P_M > P_{M2}$  the percolation of monomers is observed, and such clusters belong to the universality class of standard percolation.

Finally, we would like to remark the rich physical behavior emerging from the subtle interplay between competing processes in the case of random sequential adsorption of unlike species, as studied in this paper.

#### ACKNOWLEDGMENTS

This work was supported by UNLP, CONICET, and ANPCyT (Argentina). The authors acknowledge the kind hospitality of Professor K. Binder at the University of Mainz (Germany). F.R. acknowledges the support of CIC (Pcia. Bs. As.), Argentina.

- [1] T. L. Hill, *Statistical Mechanics* (McGraw-Hill, New York, 1956).
- [2] H. E. Stanley, *Introduction to Phase Transition and Critical Phenomena* (Oxford University Press, New York, 1971).
- [3] R. J. Baxter, *Exactly Solved Models in Statistical Mechanics* (Academic, London, 1982).
- [4] G. M. Bell and D. A. Lavis, *Statistical Mechanics of Lattice Models* (Wiley, London, 1989).
- [5] *Computational Methods in Surface and Colloid Science*, edited by M. Borówko, Surfactant Science Series Vol. 89 (Marcel Dekker Inc., New York, 2000).
- [6] A. Patrykiewicz, S. Sokotowski, and K. Binder, *Surf. Sci. Rep.* **37**, 207 (2000).
- [7] T. L. Einstein, *Chemistry and Physics of Solid Surfaces*, edited by R. Vanselow and R. Hove (Springer-Verlag, Berlin, 1982), Vol. 4.
- [8] W.H. Weinberg, *Annu. Rev. Phys. Chem.* **34**, 217 (1983).
- [9] J.J. Ramsden, *J. Stat. Phys.* **73**, 853 (1993).
- [10] E.A. Boucher, *Prog. Polym. Sci.* **6**, 63 (1978).
- [11] J.W. Evans and D.R. Burgess, *J. Chem. Phys.* **79**, 5023 (1983).
- [12] M.C. Bartelt and V. Privman, *J. Chem. Phys.* **93**, 6820 (1990).
- [13] J.W. Evans, *Rev. Mod. Phys.* **65**, 1281 (1993).
- [14] V. Privman, *Nonequilibrium Statistical Mechanics in One Dimension* (Cambridge University Press, Cambridge, 1997).
- [15] P.J. Flory, *J. Am. Chem. Soc.* **61**, 1518 (1939).
- [16] P. Schaaf and J. Talbot, *Phys. Rev. Lett.* **62**, 175 (1989).
- [17] R.D. Vigil and R.M. Ziff, *J. Chem. Phys.* **91**, 2591 (1989).
- [18] J.W. Lee, *Phys. Rev. E* **55**, 3731 (1997).
- [19] C.K. Gan and J.S. Wang, *Phys. Rev. E* **55**, 107 (1997).
- [20] B. Bonnier, *Phys. Rev. E* **56**, 7304 (1997).
- [21] B. Mellin and E.E. Mola, *J. Math. Phys.* **26**, 514 (1985).
- [22] P. Meakin and R. Jullien, *Phys. Rev. A* **46**, 2029 (1992).
- [23] R. Imbhil, *Prog. Surf. Sci.* **44**, 185 (1993).
- [24] R. Imbhil and G. Ertl, *Chem. Rev.* **95**, 697 (1995).
- [25] R.M. Ziff, E. Gulari and Y. Barshad, *Phys. Rev. Lett.* **56**, 2553 (1986).
- [26] D. Stauffer and A. Aharony, *Introduction to Percolation Theory* (Taylor and Francis, London, 1992).
- [27] A. Bunde and S. Havlin, *Fractals in Science* (Springer Verlag, Berlin, 1994).
- [28] A. Bunde and S. Havlin, in *Percolation I, Fractals and Disordered Systems* (Springer-Verlag, Berlin, 1992).
- [29] Y. Leroyer and E. Pommiers, *Phys. Rev. B* **50**, 2795 (1994).
- [30] H.S. Choi, J. Talbot, G. Tarjus, and P. Viot, *Phys. Rev. E* **51**, 1353 (1995).
- [31] N. Vandewalle, S. Galam, and M. Kramer, *Eur. Phys. J. B* **14**, 407 (2000).
- [32] G. Kondrat and A. Pekalski, *Phys. Rev. E* **63**, 051108 (2001).
- [33] J. Hoshen and R. Kopelman, *Phys. Rev. B* **14**, 3427 (1976); Ref. [28], p. 83.
- [34] R. Ziff, *Phys. Rev. Lett.* **69**, 2670 (1992).